Science and Technology Indonesia
e-ISSN:2580-4391 *p*-ISSN:2580-4405
Vol. 11, No. 1, January 2026

Research Paper

Functionalization of Titanium Dioxide Nanoparticles in Anatase-Rutile Phases and Quartz Crystal Microbalance for Humidity Sensing Materials

Laili Mardiana[1*], Baiq Nurul Fajriah[1], Rahadi Wirawan[1], Alfina Taurida Alaydrus[1], Susi Rahayu[1]

[1]*Physics Study Program, University of Mataram, West Nusa Tenggara, 83125, Indonesia*
***Corresponding author**: lailimardiana@unram.ac.id*

Abstract
A QCM (Quartz Crystal Microbalance) can be developed as a humidity sensor with a selective coating material. TiO_2 (titanium dioxide) is a metal oxide with several crystal phases: anatase and rutile phases. However, there are few studies on the crystal phase investigation of a TiO_2-based humidity sensor. Thus, this study aimed to develop a humidity sensor by functionalizing TiO_2 particles with different crystal phases. The coating materials were prepared by ultrasonication. The synthesis was conducted by mixing 7 mL of TTIP (Titanium (IV) Isopropoxide) precursor in ethanol. This solution was stirred for 30 minutes, ultrasonicated, and heated for 16 hours to make a gel. The next step was a calcination process with two different temperatures to produce different crystal phases: 500°C (anatase) and 700°C (rutile). The synthesized powders were analyzed using XRD-SEM and coated onto the surfaces of the QCMs used as the developed sensors. These sensors were tested inside a chamber using a humidity control kit and a frequency counter (humidity levels: 57% to 92%). The results show that the rutile phase has a smaller particle diameter (252.672 nm) than the anatase phase (384.589 nm). The humidity sensing examinations indicate that the anatase-phase sensor has faster response-recovery times (19 seconds and 8 seconds) than the rutile-phase sensor (28 seconds and 50 seconds). It can be concluded that TiO_2 particles in the anatase and rutile phases can be functionalized as a high-sensitivity coating material for a QCM humidity sensor.

Keywords
Humidity Sensor, Nanoparticle, Quartz Crystal Microbalance, Titanium Dioxide

Received: 16 June 2025, Accepted: 19 November 2025
https://doi.org/10.26554/sti.2026.11.1.252-260

1. INTRODUCTION

Humidity (well-known as relative humidity level) is one of the important environmental parameters in many sectors, including the industrial, agricultural, medical, and aerospace sectors (Deng et al., 2025). The importance of humidity parameters requires the need for sustainable, inexpensive, and reliable humidity sensors to meet the high demand in these industries (Farou et al., 2025). In recent years, humidity sensors have been widely developed to improve sensor sensitivity, response time, and recovery time. The most widely used humidity sensors are transistor-based (Liu et al., 2025), fiber-optic (Qi et al., 2025), MEMS (Micro Electro Mechanical System) (Gulsaran et al., 2024), and QCM (Chen et al., 2025). QCM is widely used as a sensor due to its high sensitivity at the nanogram scale, real-time measurement capabilities, and ease of modification and operation (Triyana et al., 2018). A QCM is a gravimetric crystal that produces a frequency signal proportional to the mass on its surface. QCM has unique electrodes that must be coated using various methods, such as spin coating, dip coating, and others. Therefore, QCM sensors are widely used as gas (Wang et al., 2025) and particulate matter (Budianto et al., 2021) sensors. Previous studies have confirmed that the coating material is important for increasing the selectivity and sensitivity of the QCM sensor (Tang et al., 2025).

TiO_2 is a semiconductor material that has good optical, dielectric, chemical stability, and non-toxic properties (Taha et al., 2020). The crystal structure of TiO_2 has three phases: anatase, rutile, and brookite (El Koulali et al., 2025). The advantages of these properties make TiO_2 widely used in various fields, such as electrochemistry (Sepúlveda et al., 2025), capacitors (Chernikova et al., 2025), solar cells and photocatalysts (Ding et al., 2025), and as a coating material (Irawan et al., 2024; Sun et al., 2025). TiO_2 is known to exhibit high-water-content sensitivity (and a rapid response) due to its ability to adsorb large numbers of gas-phase molecules on its surface (Chew et al., 2025). Each crystal structure has distinct properties, even though they are two distinct crystalline phases of TiO_2. Anatase is a metastable form, while rutile is the thermodynamically stable phase at room temperature and pressure. Both phases have a tetragonal crystal structure, but with different

atomic arrangements (Hossain and Ahmed, 2023).

TiO_2 can be synthesized in several ways, including the sol-gel method (Mohammed-Amine et al., 2025), the coprecipitation method (Dariz et al., 2025), the hydrolysis method (Wijekoon et al., 2025), and the ultrasonication method (Mardiana et al., 2022). The ultrasonication method is often used because it can produce uniform TiO_2 with good phase purity, crystalline structure, and a high success rate (Guo et al., 2025). The resulting TiO_2 powder can then be used for various purposes, including as a layer in a QCM.

Surface acoustic wave- or QCM-based humidity sensors that use specific coating materials, such as a TiO_2 layer, have been reported to exhibit low-to-high sensitivity (Dou et al., 2025). On the other hand, no clear study has been conducted on the crystal phase and its effect on the sensor system's static characteristics. Most previous studies have focused on the functionalization of the anatase phase. Moreover, the developed sensors are primarily used for gas sensing applications, such as nitrogen dioxide and carbon dioxide detection systems (Mardiana et al., 2022; Procek et al., 2015; Zhang et al., 2025b). Besides, the most important aspect of gas-sensing examination, especially for carbon dioxide monitoring systems, is the observation of humidity levels. It is related to water molecules in many humid or harsh environments, where they can generate a mass-loading effect (swelling) and disturb the sensor's output signal. There is limited information on the development of humidity sensors using TiO_2 nanoparticles. In line with this gap of knowledge, this study aimed to develop a humidity sensor by functionalizing TiO_2 particles with different crystal phases. This study may contribute to the development of sensor technology for environmental purposes.

2. EXPERIMENTAL SECTION

2.1 Chemicals

The first step was the synthesis of TiO_2 nanoparticles. TTIP (Sigma-Aldrich, 97%) was used as the precursor in this synthesis step via ultrasonication. This method was used due to the short duration and the ease of examining the TiO_2 nanoparticle (Chew et al., 2025). All tools were cleaned using distilled water-acetone and naturally air-dried to avoid contamination (Franzelli et al., 2024). TTIP (volume V = 7 mL) was carefully prepared inside an Erlenmeyer flask to avoid sparks due to its reactivity. The TTIP solution was placed in a container filled with water before ethanol (96%) was added as the solvent (V = 70 mL). The resulting solution was covered with aluminum foil and stirred for 30 minutes using a magnetic stirrer to produce a homogeneous solution. The next step was ultrasonication with a frequency (f) of 40 kHz for 4 hours. Then, this solution was heated to 80°C for 16 hours to produce a gel mixture. The final step was a calcination process for 3 hours with two temperature variations: (a) 500°C (anatase) and (b) 700°C (rutile) to make TiO_2 powder with different phases (Lirong et al., 2022). XRD and SEM-EDS were used to characterize the resulting TiO_2 powder and determine its crystal structure and particle size distribution.

2.2 Quartz Crystal Microbalance

This study used QCM crystals (AT-cut type) as the developed sensor (purchased from PT. Great Microtama Electronics Indonesia). These crystals were purchased without any coating material (bare sensors). The crystals have silver electrodes with the initial frequency of 5 MHz.

2.3 Sensor Development Procedure

TiO_2 solution was prepared (0.1 molar, aquabides were used as the solvent) and dropped on the surface of the QCM using a vacuum spin coater (V = 1 μL, Weiyi, model VTC-100). This coating step was conducted with a rotation of 500 RPM (for 5 seconds) and 1500 RPM (for 60 seconds). Then, the coated QCM was dried at room temperature and tested as a humidity sensor using a frequency meter (High Resolution Counter – Aditeg, model AFC8240). The TiO_2-coated QCM sensor was developed as a novel humidity sensor. This sensor was tested inside a chamber with a nebulizer to gradually control and maintain the humidity level (57% - 92%). This test was also calibrated using a comparator device, while the frequency shift (f) was recorded using a frequency meter (Figure 1) (Mardiana et al., 2024).

2.4 Characterization

The sensor surface was examined using a SEM-EDS (JEOL, model JCM7000). This examination was conducted to determine the particle size distribution. The crystal structure was analyzed by XRD (Qadri et al., 2024; Septriansyah et al., 2025). Sensor performance was determined by evaluating the response-recovery times displayed on a frequency meter and an oscilloscope (Eduscope, model 3000) (Qian et al., 2025; Zhang et al., 2025a).

3. RESULTS AND DISCUSSION

3.1 Crystal Structure Analysis

The results of the XRD analysis are interpreted as a diffractogram consisting of lines or peaks with different intensities and positions. The results show typical TiO_2 peaks. As shown in Figures 2a-b and Table 1, TiO_2 crystals synthesized by ultrasonication exhibit characteristic diffraction peaks at 2θ and d values that match those reported in the JCPDS (Joint Committee on Powder Diffraction Standards). The first sample, anatase crystal structure, is formed during calcination at temperatures ranging from 120° to 500°C over 3 hours. The rutile crystal structure forms when the calcination temperature is increased to 700°C (Lirong et al., 2022). Based on the JCPDS analysis, TiO_2 calcined at 500°C has formed an anatase phase (JCPDS no. 21-1272). In addition, TiO_2 calcined at 700°C is confirmed to be in the rutile phase (JCPDS no. 21-1276). Figure 2 shows the suitability of the crystal plane orientation in JCPDS with the synthesized TiO_2. The hkl value indicates the suitability of the crystal plane orientation.

The corresponding peak values for the anatase phase at an angle of 2θ are: 25.139° (101); 37.776° (004); 47.874° (200); 53.891° (105); 54.897° (211); 62.644° (204); 68.892°

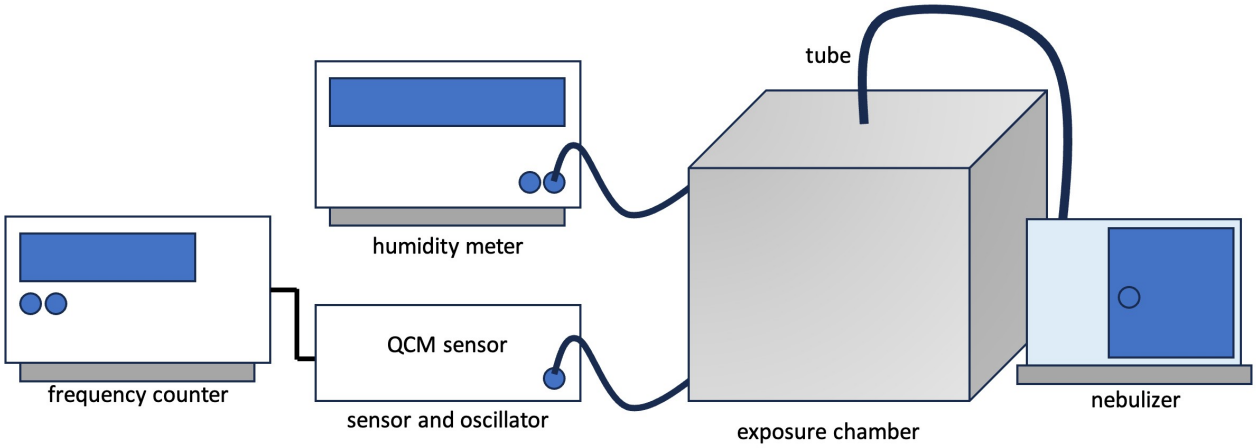

Figure 1. Sensor Examination Inside an Exposure Chamber

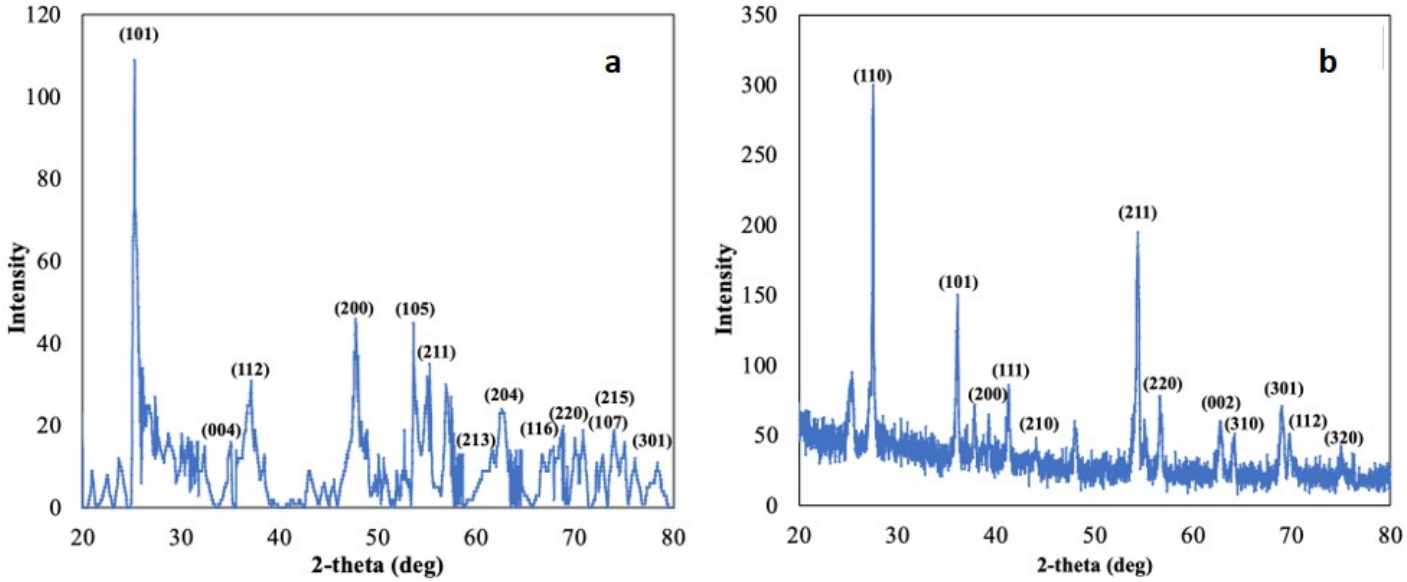

Figure 2. XRD Pattern Results (TiO_2) in: (a) Anatase and (b) Rutile Phases

Table 1. XRD Examinations in Different Crystal Phases

Phases	Crystal Structures	2θ	hkl	d-spacing (Å)
Anatase (JCPDS 21-1276)	Tetragonal	25.139440	101	3.54246
		37.776808	004	2.38149
		47.874320	200	1.90010
		53.891850	105	1.70129
		59.897900	211	1.67249
		62.644170	204	1.48300
Rutile (JCPDS 21-1272)	Tetragonal	27.513120	110	3.24199
		36.069760	101	2.49014
		39.225700	200	2.29680
		41.251250	111	2.18854
		44.047710	210	2.05587
		54.324020	211	1.68877

(116); 70.578° (220); 73.995° (107); 75.021° (215); and 76.685° (301). The rutile phase corresponding to the peaks in JCPDS no. 21-1276 are 27.513° (110); 36.069° (101); 39.225° (200); 41.251° (111); 44.048° (210); 54.324° (211); 56.609° (220); 62.774° (002); 64.085° (310); 68.982° (301); 69.805° (112); and 75.008° (320).

The highest intensity of the rutile phase is located at position 2θ (27.513°) of 300, which is the peak of the TiO_2 crystal. As for the anatase phase, the highest intensity value is 110 at position 2θ (25.139°). Overall, the rutile phase is more intense than the anatase phase. The intensity of a crystal structure indicates good crystal regularity, so that its atoms are arranged regularly. Conversely, low intensity indicates that the atoms in the structure are not highly ordered. At high intensity, X-rays will diffract more efficiently. As found in this study, the rutile crystal structure formed at a calcination temperature of 700°C. The anatase phase transformed to rutile at 600-750°C. The highest purity is obtained at a calcination temperature of 700°C. The anatase and rutile crystal structures are highly stable, making them widely used across various fields. In contrast, the brookite crystal structure is poorly stable and difficult to form. This increasing temperature will change the crystal structure in the anatase phase (orthorhombic to tetragonal). The orthorhombic crystal structure shows higher sensitivity to H_2O molecules. In this case, the crystal structure exhibits greater hydrophilic properties than the tetragonal structure.

3.2 Particle Size Distribution

The morphology of a particle is the shape and characteristics of a material. SEM-EDS examinations were carried out to determine the particle size distribution and TiO_2 content of the synthesized results. The samples characterized were TiO_2 powders that had undergone grinding and sieving. According to the analysis, the anatase crystal phase (Figure 3a) shows a size distribution of 384.589 ± 59.507 nm. Besides, the rutile crystal phase (Figure 3b) has a particle size of 252.672 ± 24.669 nm.

The particle distribution in the anatase phase is more uniform than in the rutile phase. Both TiO_2 crystal phases have particle sizes centered at 200-300 nm. The rutile crystal phase contains more nano-sized particles than the anatase phase. These particle sizes were related to the duration and temperature of the calcination process. A longer calcination time results in a smaller particle size and a more uniform particle distribution. The particle size and distribution will affect the performance of the QCM sensor as a humidity sensor. Small particles increase the surface-to-volume ratio, thereby enhancing water vapor adsorption on the QCM sensor (Wang et al., 2025). In addition, smaller particles can form a more uniform layer and are better at measuring mass changes caused by humidity.

The next analysis was the EDS examination (Figure 4). EDS testing was conducted to determine the TiO_2 content, which was interpreted as a spectrum. The spectrum shows several peaks corresponding to the elements that comprise the analyzed sample. The titania (Ti) and oxygen (O) elements are the main elements of the synthesized TiO_2. In addition, there are copper (Cu) and niobium (Nb) elements that the nature of the stub substrate might cause. The EDS spectrum in Figure 4a shows the elements present in the anatase phase of TiO_2. The Ti element is 72.18 ± 0.79%, which is higher than O (18.64 ± 0.76%), Cu (3.93 ± 0.41%), and Nb (5.26 ± 0.21%). Besides, Figure 4b shows the elements found in the rutile phase of TiO_2. The detected elements in the rutile phase are Ti (70.96 ± 0.80%), O (17.26 ± 0.74%), Cu (5.51 ± 0.48%), and Nb (6.27 ± 0.23%).

The compounds produced by this synthesis are listed in Table 2. Both phases produce the same three compounds: TiO_2 (main compound), copper oxide (CuO), and niobium (V) oxide (Nb_2O_5).

The EDS test results showed that the synthesis of TiO_2 in the anatase phase of TTIP produced TiO_2 of 90.67 ± 1.03%, followed by other compounds such as CuO (3.71 ± 0.38%) and Nb_2O_5 (5.51 ± 0.22%). The synthesis in the rutile phase produced TiO_2 of 88.23 ± 0.99%. This phase also produced CuO (5.15 ± 0.45%) and Nb2O5 (6.62 ± 0.24%). These values indicate that the synthesis of TiO_2 with TTIP precursor using the ultrasonication method has been successfully carried out. This is in line with a previous study that used ultrasonication for TiO_2 synthesis. This study shows a uniform morphology, good phase purity, a high-crystallinity structure, a high synthesis success rate, and low production costs. Moreover, the decrease in mass in TiO_2 calcined at temperatures of 500°C and 700°C can occur due to the decomposition of impurity compounds lost in the form of gas or dehydration of crystal water and water adsorbed on TiO_2.

3.3 Sensor's Performance Test

The TiO_2-coated QCM sensor is used as the humidity sensor. This novel sensor was tested using frequency-shift measurements during a humidity change. According to the results, the frequency changes increase with increasing humidity, indicating the presence of water molecules adsorbed on the sensor. A more humid condition indicates more water molecules sticking to the QCM. Therefore, the more humid the air, the greater the frequency changes on the QCM sensor. TiO_2 has strong hydrophilic properties, allowing it to absorb large amounts of water molecules from the gas phase on its surface. At room temperature, water vapor adsorbs to form a multilayer on the QCM sensor surface. In line with this, a large amount of water, which is dissociated by strong bonds, can be well adsorbed. This interaction causes the first layer to dissociate, forming hydroxide ions (OH^-). After the first layer, molecular physiosorbed water with Van der Waals interactions will form hydrogen bonds (Lirong et al., 2022).

Figure 5 presents the sensor's performance test results. These figures indicate that both anatase- and rutile-phase sensors exhibit good performance. The anatase phase sensor can detect a humidity level of 72%, with a response time of 1-2 seconds (average response time = 1.5 seconds). As shown in

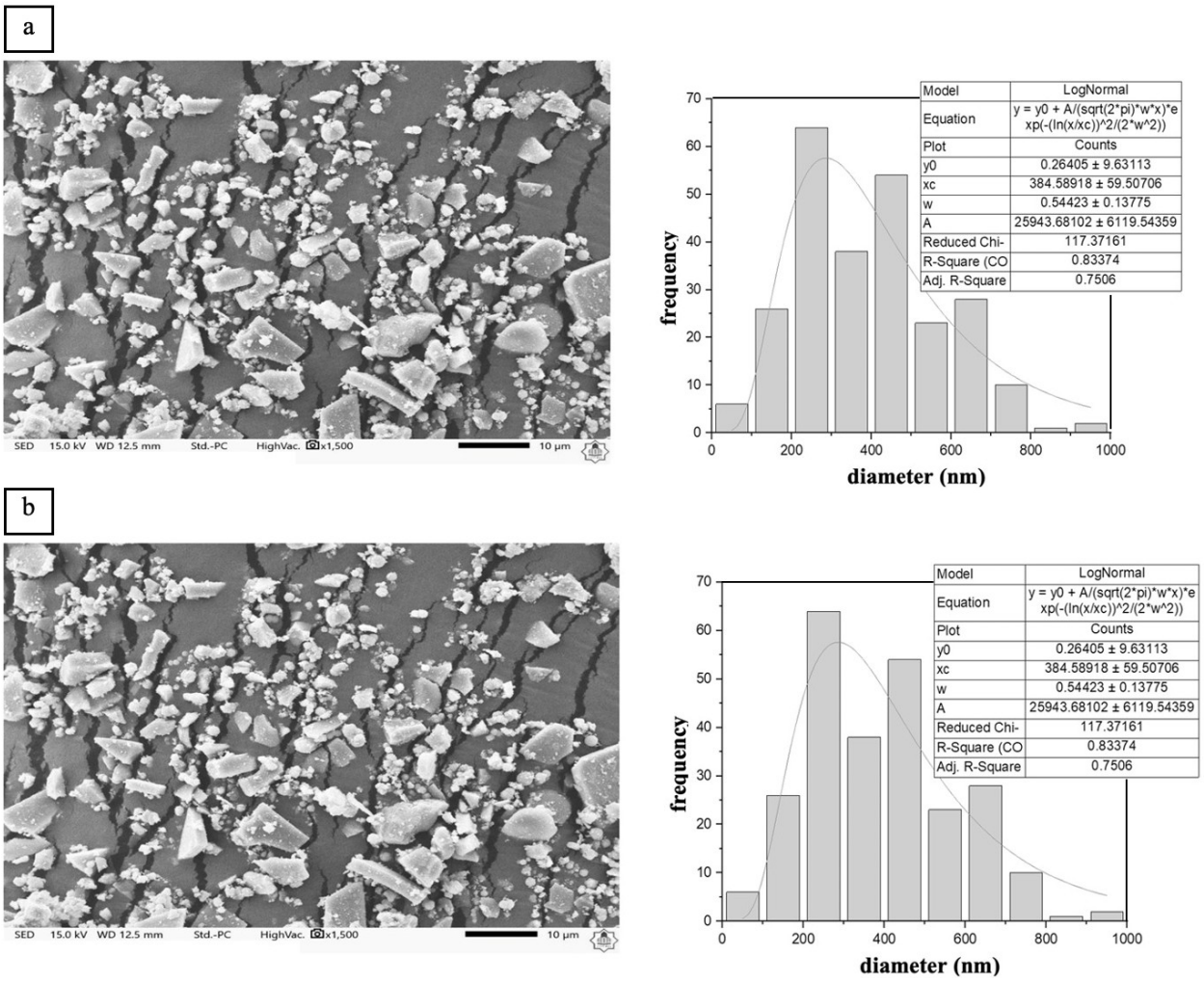

Figure 3. Particle Size Distribution Analysis (using SEM) of the (a) Anatase and (b) Rutile Phases (mag. = 1500×)

Table 2. EDS Examinations in Different Crystal Phases

Anatase			
Chemical Formula	Line	%Mass	%Mol
O	K	–	–
TiO_2	K	90.67 ± 1.03	94.36 ± 1.03
CuO	K	3.71 ± 0.38	3.88 ± 0.40
Nb_2O_5	L	5.51 ± 0.22	1.76 ± 0.07
Rutile			
Chemical Formula	Line	%Mass	%Mol
O	K	–	–
TiO_2	K	88.23 ± 0.99	94.36 ± 1.03
CuO	K	5.15 ± 0.45	3.88 ± 0.40
Nb_2O_5	L	6.62 ± 0.24	1.76 ± 0.07

Figure 5a, at the 164th measurement time, the anatase phase sensor undergoes a recovery to its initial frequency. Hence, the sensor's recovery time is about 8 seconds. Additionally, Figure 5b shows that the rutile phase sensor performs well at 78% RH. This sensor starts to work actively at the 20th (humidity = 57%) to 25th (humidity = 59%) measurement time, so the response time of this rutile phase sensor is about 4 seconds. At 186-188 seconds, this sensor recovers to its initial frequency, resulting

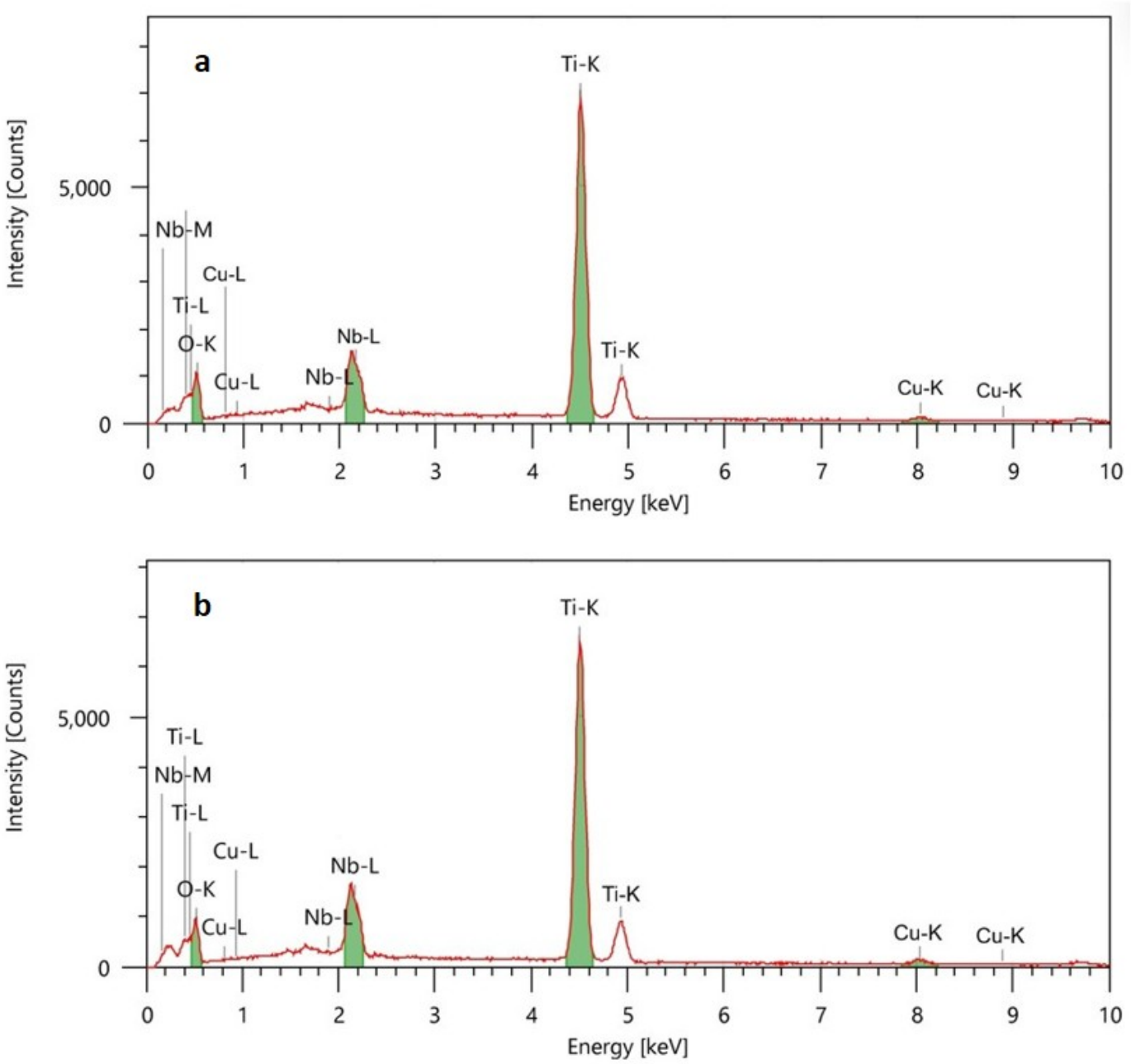

Figure 4. EDS Analysis Results in: (a) Anatase and (b) Rutile

in a recovery time of about 14 seconds.

Based on Figure 5, the QCM sensor coated with the rutile phase can measure higher relative humidity than one coated with the anatase phase. This figure also interprets that the rutile sensor has a longer response time than the anatase phase. These differences may be related to differences in particle size distribution. The rutile crystal phase has a particle size of 252.672 ± 24.669 nm, while the anatase crystal phase has a particle size of 384.589 ± 59.507 nm. This particle size will affect the quality of H_2O adsorption-desorption on the surface of the sensors (Sun et al., 2025). In addition, the distribution of TiO_2 particles deposited on the surface of the QCM sensor with a denser rutile crystal structure also results in a better sensor response to humidity.

The denser, more stable rutile crystal structure results in a longer recovery time for the TiO_2-coated QCM sensor in the rutile phase than in the anatase phase. The rutile phase has a tetragonal crystal form, while the anatase phase has an orthorhombic crystal structure. In this parameter, the tetragonal crystal form provides more uniform and consistent proper-

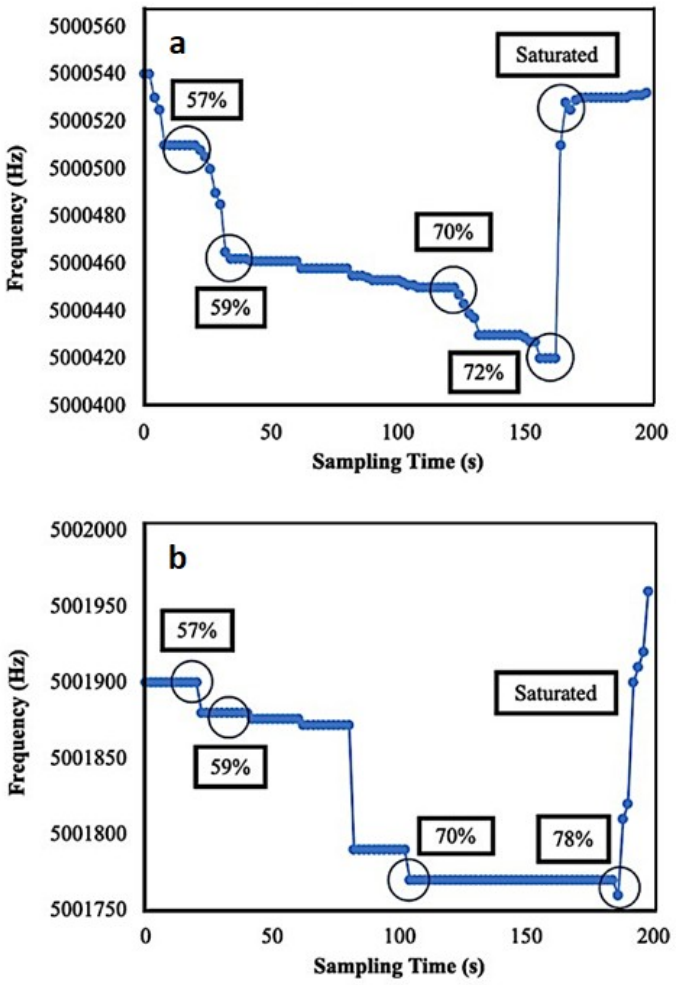

Figure 5. Frequency Shifts During the Humidity Test: (a) Anatase and (b) Rutile

ties than orthorhombic crystals. In addition, the rutile phase's structure will produce durable, more environmentally resistant properties, including resistance to humidity. In contrast, the anatase phase will undergo faster structural changes, thereby affecting its performance as a layer in the humidity sensor. Thus, this statistic can directly influence the sensor performance, as found in the rutile phase.

4. CONCLUSIONS

Synthesis of TiO_2 by ultrasonication has been successfully carried out at calcination temperatures of 500°C (anatase phase) and 700°C (rutile phase), yielding TiO_2 of 90.67 ± 1.03% and 88.23 ± 0.99%, respectively. Variation of calcination temperature in TiO_2 synthesis affects the crystal structure formed. At a calcination temperature of 500°C, an anatase crystal structure is produced, and at a temperature of 700°C, a rutile crystal structure is produced. The functionalized TiO_2 used as the QCM coating material exhibits good humidity-sensing properties in both the anatase and rutile crystal phases. The humidity sensing examinations indicate that the anatase-phase sensor has faster response-recovery times (19 and 8 seconds) than the rutile-phase sensor (28 and 50 seconds). It can be concluded that TiO_2 particles in the anatase and rutile phases can be functionalized as a high-sensitivity coating material for a QCM humidity sensor.

5. ACKNOWLEDGMENT

All authors wish to thank the Institute for Research and Community Services (LPPM) of the University of Mataram for the research funding (contract number 1260/UN18.L1/PP/2024).

REFERENCES

Budianto, A., A. Y. P. Wardoyo, Masruroh, H. A. Dharmawan, and M. Nurhuda (2021). Performance Test of an Aerosol Concentration Measurement System Based on Quartz Crystal Microbalance. *Journal of Physics: Conference Series*, **1811**; 1–8

Chen, Q., Y. Yao, J. Ao, X. Yu, D. Wu, M. Shou, R. Li, and P. Yang (2025). Advances in Quartz Crystal Microbalance Relative Humidity Sensors: A Review. *Measurement*, **243**; 116415

Chernikova, A. G., N. A. Sizykh, I. V. Zabrosaev, and A. M. Markeev (2025). TiN/HZO/TiN Ferroelectric Capacitors With TiO_2 Insets: Critical Difference Between Top and Bottom Interface Modification. *Surfaces and Interfaces*, **62**; 106135

Chew, Y. B., C. M. Ling, P. W. Koh, C. S. Chew, and S. L. Lee (2025). Sonochemical Synthesis of Rutile Phase Copper-Doped Titanium Dioxide Coating on Fabric and Its Application in Antibacterial Testing of *Staphylococcus aureus*. *Science and Technology Indonesia*, **10**(2); 605–613

Dariz, M. A., J. É. Marmentini, G. L. Colpani, M. A. Fiori, A. A. C. Recco, O. C. Alves, M. Z. Fidelis, and R. Brackmann (2025). Exploring the Unique Physicochemical Properties of Fe_3O_4@TiO_2-Nd Magnetic Nanocomposites Synthesized via Hydrothermal Coprecipitation. *Journal of Magnetism and Magnetic Materials*, **614**; 172752

Deng, Y., Y. Shi, Q. Zeng, C. Xu, L. Fu, and B. Lin (2025). Facile Preparation of Inexpensive Polysaccharides-Based Antibacterial Sensor for All-Round Monitoring of Humidity and Temperature in Grain Storage. *Chemical Engineering Journal*, **507**; 160514

Ding, X., Q. Yu, H. Xue, W. Zhang, H. Ren, and J. Geng (2025). Photochemical Behavior of Extracellular Polymeric Substances in Intimately Coupled TiO_2 Photocatalysis and Biodegradation System. *Bioresource Technology*, **416**; 131752

Dou, Y., C. Li, W. Luo, L. Qian, L. Wang, D. Li, H. Li, and M. Li (2025). Surface Acoustic Wave Relative Humidity Sensor Based on GO/TiO_2 Sensitive Film. *Sensors and Actuators A: Physical*, **365**; 114906

El Koulali, F., M. Ouzzine, L. Cano-Casanova, M. C. Román-Martínez, and M. A. Lillo-Ródenas (2025). Use of the HighScore Plus Software for an Easy and Complete Quan-

tification of the Anatase, Brookite, Rutile, and Amorphous Phase Content in TiO_2. *Chemistry of Inorganic Materials*, **5**; 100086

Farou, M., A. Djellad, S. Chiheb, H. Lalaymia, B. Rekik, and P. O. Logerais (2025). Quantification of the Impact of Irradiance, Heat, Humidity, and Cyclic Temperature on the Aging of Photovoltaic Panels: A Case Study in Algeria. *Energy Reports*, **13**; 642–652

Franzelli, B., J. Bonnety, J. Yi, Y. Ogata, A. Cuoci, and C. Betrancourt (2024). Numerical Simulations of TiO_2 Production in a Laminar Coflow H_2/Ar/TTIP Diffusion Flame: Comparison With Experiments and Parametric Sensitivity Study. *Proceedings of the Combustion Institute*, **40**; 105599

Gulsaran, A., B. Azer, R. Saritas, S. Kocer, Y. S. Shama, S. Rahmanian, H. Mouharrar, R. Abdelrahman, E. Abdel-Rahman, and M. Yavuz (2024). High Sensitivity, Thermal Noise-Driven Aluminum-Based Resonant MEMS Humidity Sensor. *Sensors and Actuators A: Physical*, **378**; 115844

Guo, Z., Y. Chen, N. Wang, Y. Xu, Q. Zhao, Z. Hou, G. Gao, Y. Kang, and H. Zhan (2025). Ultrasonic-Assisted MoS_2/GO/TiO_2 Ceramic Coatings: Enhancing Anti-Friction Performance Through Dual-Interface Optimization. *Ultrasonics Sonochemistry*, **112**; 107180

Hossain, S. and S. Ahmed (2023). Easy and Green Synthesis of TiO_2 (Anatase and Rutile): Estimation of Crystallite Size Using Scherrer Equation, Williamson-Hall Plot, Monshi-Scherrer Model, Size-Strain Plot, Halder-Wagner Model. *Results in Materials*, **20**; 100492

Irawan, D., Azhar, K. Ramadhan, A. Marwin, and A. Marwan (2024). Numerical Study of Early Detection of Tuberculosis Infected With High Sensitivity Plasmonic Sensor. *Science and Technology Indonesia*, **9**(1); 94–102

Lirong, Y., L. Xiaoyu, W. Chunmei, L. Zhigang, and F. Xiaoxin (2022). Influence of Calcination Temperatures on the Anatase and Rutile Mixed Phase Composition and Photocatalytic Activity of the Carbon Doped Mesoporous TiO_2. *Optical Materials*, **133**; 112997

Liu, R., Z. Wu, Q. Li, S. Shamim, and L. Ba (2025). Fully Printed Field-Effect Transistor Humidity Sensor With Chitosan/Polyvinyl Alcohol/Nano Carbon Powder for Enhanced Moisture Sensitivity. *Talanta*, **287**; 127679

Mardiana, L., A. Y. P. Wardoyo, Masruroh, and H. A. Dharmawan (2022). Synthesis TiO_2 Using Sonochemical Method and Responses the CO_2 Gas of the Nanoparticle TiO_2 Layers on the QCM Sensor Surfaces. *Journal of Physics: Conference Series*, **2165**; 012014

Mardiana, L., A. Y. P. Wardoyo, Masruroh, and H. A. Dharmawan (2024). The Effect of Humidity Levels on Carbon Dioxide Gas Concentration Measurement Using a Titanium Dioxide-Coated Quartz Crystal Microbalance. *Evergreen*, **11**(1); 137–142

Mohammed-Amine, E., B. Kaltoum, E. M. El Mountassir, A. T. Abdelaziz, R. Stephanie, L. Stephanie, P. Anne, W. W. C. Pascal, M. M. Alrashed, and R. Salah (2025). Novel Sol-Gel Synthesis of TiO_2/$BiPO_4$ Composite for Enhanced Photocatalytic Degradation of Carbamazepine Under UV and Visible Light: Kinetic, Identification of Photoproducts and Mechanistic Insights. *Journal of Water Process Engineering*, **70**; 107098

Procek, M., A. Stolarczyk, T. Pustelny, and E. Maciak (2015). A Study of a QCM Sensor Based on TiO_2 Nanostructures for the Detection of NO_2 and Explosives Vapours in Air. *Sensors*, **15**(4); 9563–9581

Qadri, L. A., G. A. Abelta, M. Febrina, A. Rajak, S. Maulana, M. A. Asagabaldan, and T. Taher (2024). Effect of Calcination Temperature on the Adsorption Performance of Tanggamus Natural Zeolite for Ammonium Removal From Shrimp Pond Wastewater. *Science and Technology Indonesia*, **9**(1); 198–206

Qi, Y., J. Li, Y. Chen, B. Zhu, X. Zhou, X. Xiao, Z. Gu, J. Qian, C. He, M. Lai, Y. Ma, and B. Liu (2025). Differential Fiber Optic Humidity Sensor Based on Superhydrophilic SiO_2 /Polyethylene Glycol Composite Film With Linear Response. *Optical Fiber Technology*, **90**; 104150

Qian, Y., J. Zou, X. Jiang, J. Wang, J. Zhou, C. Cheng, X. Zhang, W. He, Q. Jin, and J. Jian (2025). Improving CO_2 Resistance in High-Temperature Humidity Sensors Using $LaFeO_3$ Sensing Electrodes. *Sensors and Actuators B: Chemical*, **431**; 137423

Septriansyah, V., S. Saloma, S. A. Nurjannah, A. Saggaff, A. P. Usman, and S. P. Ngian (2025). Effect of the Nano-Silica Addition on the Mechanical Properties of Polymer Concrete. *Science and Technology Indonesia*, **10**(1); 9–17

Sepúlveda, M., H. Sopha, V. Cicmancova, L. Hromadko, and J. M. Macak (2025). TiO_2 Nanotubes Grown on Ti and Ti_6Al_4V Alloy Spheres by Bipolar Anodization. *Electrochemistry Communications*, **170**; 107855

Sun, S., C. Zhao, Z. Zhang, D. Wang, X. Yin, J. Han, J. Wei, Y. Zhao, and Y. Zhu (2025). Highly Selective QCM Sensor Based on Functionalized Hierarchical Hollow TiO_2 Nanospheres for Detecting PPB-Level 3-Hydroxy-2-Butanone Biomarker at Room Temperature. *Chinese Chemical Letters*, **36**; 109939

Taha, S., S. Begum, V. N. Narwade, D. I. Halge, J. W. Dadge, M. P. Mahabole, R. S. Khairnar, and K. A. Bogle (2020). Development of Alcohol Sensor Using TiO_2 -Hydroxyapatite Nano-Composites. *Materials Chemistry and Physics*, **240**; 122228

Tang, K., X. Ding, X. Yu, J. Lu, F. Liu, H. Li, and X. Chen (2025). High Fundamental Frequency QCM Humidity Sensor Based on C_{60}-OH/ Ti_3C_2TX Nanocomposite With Superior Response. *Sensors and Actuators B: Chemical*, **426**; 137014

Triyana, K., A. Sembiring, A. Rianjanu, S. N. Hidayat, R. Riowirawan, T. Julian, A. Kusumaatmaja, I. Santoso, and R. Roto (2018). Chitosan-Based Quartz Crystal Microbalance for Alcohol Sensing. *Electronics*, **7**(9); 1–11

Wang, L., J. Song, and C. Yu (2025). Recent Progress on Mass-Sensitive Gas Sensors for Environmental and Industrial Applications. *Measurement*, **249**; 117039

Wijekoon, S. H. D. P., M. Shimomura, T. Kawaguchi, N. Shimosako, N. Sakamoto, and N. Wakiya (2025). Smooth TiO_2 Thin Film Fabrication by On-Site Controlled Hydrolysis of Alcohol-Titanium Alkoxide Mixtures. *Surfaces and Interfaces*, **58**; 105755

Zhang, H., X. Xu, J. Lu, M. Huang, Y. Wang, Z. Feng, and Y. Wang (2025a). Flexible Non-Contact Printed Humidity Sensor: Realization of the Ultra-High Performance Humidity Monitoring Based on the MXene Composite Material. *Sensors and Actuators B: Chemical*, **432**; 137481

Zhang, Y., D. Zhang, H. Zhang, Y. Wu, W. Liu, Z. Wang, and G. Xi (2025b). Nanoflower-Like Titanium Dioxide Modified Ethyl Cellulose-Based QCM Humidity Sensor With Low-Hysteresis for Wearable Respiratory Monitoring. *Sensors and Actuators B: Chemical*, **443**; 138286

